https://doi.org/10.1016/j.enconman.2019.04.016

Performance analysis of a novel SOFC-HCCI engine hybrid system coupled with metal hydride reactor for H_2 addition by waste heat recovery

Zhen Wu[1,2], Peng Tan[2,3], Pengfei Zhu[1], Weizi Cai[2], Bin Chen[2], Fusheng Yang[1], Zaoxiao Zhang[1,4], E. Porpatham[5,*], Meng Ni[2,*]

[1]Shaanxi Key Laboratory of Energy Chemical Process Intensification, School of Chemical Engineering and Technology, Xi'an Jiaotong University, Xi'an, China

[2]Building Energy Research Group, Department of Building and Real Estate, The Hong Kong Polytechnic University, Hong Kong, China

[3]Department of Thermal Science and Energy Engineering, University of Science and Technology of China, Hefei 230026, Anhui, China

[4]State Key Laboratory of Multiphase Flow in Power Engineering, Xi'an Jiaotong University, Xi'an, China

[5]Automotive Research Centre, School of Mechanical Engineering, Vellore Institute of Technology, Vellore, India

*Corresponding author, Email: meng.ni@polyu.edu.hk(M Ni)

porpatham.e@vit.ac.in (E Porpatham)

Abstract: A novel SOFC-HCCI engine hybrid power generation system fueled with alternative fuels is proposed and modeled in this paper. The steady-state modelling shows that it is feasible to use SOFC anode off-gas as the downstream HCCI engine fuel for additional power generation under certain fuel utilization and operating temperature. Through parametric and exergy analyses, it is found that the hybrid system without additional H_2 can achieve a net electrical efficiency of approximately 59% and an exergy efficiency of 57%, slightly higher than the SOFC-GT hybrid system. In this hybrid system, the components of HCCI engine and its exhaust gas dominate the exergy destruction, which contributes nearly 75% but has a relatively low contribution to the total power. Based on this, the methods of recycling exhaust gas waste heat to drive hydrogen desorption of metal hydride as H_2 addition for HCCI engine and H_2 recirculation for SOFC anode off-gas are suggested to significantly improve the system overall efficiency due to the consideration of thermal efficiency. The high overall efficiency up to 79.54% and fuel flexibility demonstrate that the novel hybrid system is a promising energy conversion system.

Keywords: Fuel cell; Engine; Hybrid power system; Metal hydride; Exergy analysis

Nomenclature

Abbreviation

CLHP	chemical looping hydrogen production
DC/AC	direct current to alternating current
DIR	direct internal reforming
FC	fuel cell
GT	gas turbine
HCCI	homogeneous charge compression ignition
HEX	heat exchanger
HyT	H_2 storage tank
IC	internal combustion
LHV	lower heat value
MH	metal hydride
MHR	metal hydride reactor
NG	natural gas
R-PEMFC	reform-PEMFC

SI	spark ignition
SOFC	solid oxide fuel cell
WGS	water gas shift

Symbols

A_{cell}	fuel cell area, m^2
E_T^0	standard reversible voltage for H_2, V
Ex	exergy, kW
F	Faraday constant, C mol^{-1}
h	specific enthalpy, J mol^{-1}
I	current, A
J	current density, A m^{-2}
K	reaction equilibrium constant
$\dot{m}_{H_2}$	hydrogen molar mass, kmol s^{-1}
P	power, kW
p	pressure, bar
Q_{loss}	heat loss of the fuel cell, kW
R_g	universal gas constant, J K^{-1} mol^{-1}
T	temperature, K
U_{ir}	irreversible voltage of the fuel cell, V
y	component concentration, mol L^{-1}
ϕ	mass flow, kg s^{-1}

μ_{fuel} fuel utilization

η energy efficiency

ζ exergy efficiency

ΔH reaction enthalpy, J mol^{-1}

Subscript

a anode

as ash

c cathode

cell fuel cell

comb combustion

comp compressor

DC direct current

EN energy

exh exhaust gas

fu fuel gas

in inlet

ISC isentropy of compressor

IST isentropy of turbine

MEC mechanical efficiency of compressor

MET mechanical efficiency of turbine

n-rec non-reacting gas

ox	oxidant
out	outlet
Pre-re	pre-reforming
ref	reference
reform	reforming

1. Introduction

Sustainable development of human society has reached consensus all over the world. In the energy field, an efficient and clean energy conversion way is viewed to be effective and crucial for achieving sustainable development [1-3]. With the rapid development of modern countries, the energy consumption increases dramatically, and the environmental issues such as global warming and pollutant emissions become serious. In this context, innovative technologies for energy conversion are in urgent demand for conventional conversions of fossil fuels to meet the requirements of ultra-high conversion efficiency and ultra-low environmental impact in the meanwhile [4,5].

As is well known, internal combustion (IC) engine is still the most important energy utilization pathway to convert fossil fuels into power. Actually, the technology of IC engine generally brings about exhaust emission pollution to the environment and also has relatively low energy conversion efficiency (30%~40%) [6-8]. In order to improve efficiency and simultaneously reduce emission, extensive efforts have been carried out in recent decades. For example, our previous study [9,10] reported that the addition of H_2 helps to improve the brake thermal efficiency and simultaneously leads to lower hydrocarbon (HC), CO, and NOx emission from spark ignition (SI) engine fueled by natural gas (NG) or biogas. However, the maximum efficiency (30.2%) is still low and needs further improvement for practical applications. Generally, the low thermal efficiency is attributed to the exhaust and loss of waste heat produced from the combustion process. Thus, the waste heat recovery is an effective approach to improve the thermal efficiency of the IC engine. Accordingly, innovative technologies which can achieve both power generation and waste heat recovery, have been attracting increasing attention.

Among various innovative technologies, fuel cells (FCs) usually have ultra-high conversion efficiency and near-zero emissions as the fuel is oxidized by electrochemistry to generate electricity and heat without combustion [11-15]. Because of the unique characteristic, the FC power technology is regarded as a high-efficiency energy conversion system. Moreover, the electrochemical reaction occurred in FCs is highly exothermic with the reaction heat of 242 kJ/mol [16], indicating that a large amount of heat is released and can be utilized to drive bottomed thermodynamic cycles such as Rankine, Brayton, and Otto cycles at high operating temperatures. In this case, the combination of FCs and engines into hybrid power systems can not only adequately utilize waste heat to improve the energy conversion efficiency, but also extend the power range to facilitate practical applications. Especially, coupling solid oxide fuel cell (SOFC) can achieve the theoretical conversion efficiency up to more than 70% [17,18], nearly twice larger than the standalone IC engine due to the high operating temperature of SOFC. In addition, the high operating temperature enables the hybrid power system to use a variety of fuels, such as CH_4, biogas, NG, and petroleum gas, which are cheaper and easier to manage than pure H_2. This is because that the direct internal reforming (DIR) and water gas shift (WGS) reactions can take place inside the SOFC anode to convert the hydrocarbon fuel and CO into hydrogen in the presence of water and high temperature.

In fact, SOFC-GT (gas turbine) hybrid power system has been primarily investigated in recent years [19]. It has been successfully proven that the combination of SOFC and GT facilitates the improvement of electrical efficiency and the reduction of capital costs [20-23]. The optimized SOFC-GT hybrid system was reported to have an electrical efficiency of about 66%, which is significantly higher than the initial GT power plant, and reduce approximately 30% of the capital costs [24]. Consequently, SOFC-GT hybrid power systems are considered as potential next-generation high-efficiency energy conversion devices. However, the capacity of SOFC power generation is currently less than the order of magnitude of MWs (the general power capacity of GT). Compared with GT, IC engine usually has much lower power generation capacity, which is in the order of magnitude of kWs. Consequently, a SOFC-IC engine hybrid power system is more efficient and economical than a SOFC-GT system. Recently, Choi et al. [25] experimentally investigated the feasibility of using SOFC anode off-gas as the fuel of IC engine to generate power. They found that the engine can yield a significant amount of power with 25%-30% gross indicated efficiency while emit very low NO_x emissions. The experimental results confirmed that it is feasible to use IC engine as the bottoming cycle in a SOFC-IC engine hybrid power system. Park et al. [26] carried out a comparison study on the performance between a SOFC-IC engine and a SOFC-GT hybrid power system. They concluded that the SOFC-IC engine hybrid power system has a 0.9% efficiency improvement and a 7.6% LCOE (levelized cost of energy) reduction compared with the SOFC-GT system. It is worth noting that the external reformer prior to SOFC is heated by an additional heat exchanger rather than an internal waste heat recovery in the reported SOFC-IC engine layouts. Kang et al. [27] further integrated the components of SOFC, reformer, heat exchanger, engine, and blower together into a SOFC-engine hybrid system and established the dynamic model considering the anode off-gas variation. With an increase of the SOFC power, besides the large overshoot behavior of SOFC itself, small overshoot behavior appears in the engine power generation. In the latest report, Lee et al. [28] evaluated the exergetic and exergoeconomic performance of a SOFC-engine hybrid power system. They found that the IC engine component dominates the largest exergy destruction and the SOFC stack has the highest exergoeconomic factor of 93% in the hybrid system.

These research results indicate that the SOFC-IC engine hybrid power generation system is a potential conversion device with high efficiency and low cost. However, the power ratio of IC engine in the above-mentioned SOFC-engine hybrid systems is still too low (~10%). Therefore, the operating strategy of power distribution between SOFC and IC engine for performance optimization has not yet been reported so far. Actually, the power distribution is crucial for the performance optimization of the hybrid power system [29]. Additionally, the high degree of system complication indicates that an elaborated operation strategy is required for the SOFC-IC engine hybrid power generation system. Therefore, it is essential to study the effect of power distribution between SOFC and engine on the performance for achieving optimal operation strategy for the SOFC-IC engine hybrid power generation system, which has not been reported in the previous studies.

In the present study, the steady-state model of the NG fueled SOFC-engine hybrid system is first established. Then, the parametric and exergy analyses of the hybrid system are performed to find out the optimization strategy. Herein, three cases, including no H_2 addition, H_2 addition by H_2 storage tank (HyT), and H_2 addition by metal hydride reactor (MHR), are considered for the engine fuel and compared to regulate the power distribution between SOFC and engine for performance optimization. Besides, the effect of SOFC anode H_2 recirculation on the system performance is also discussed. The results contribute to the development of optimization rule and operation strategy for the SOFC-IC engine hybrid power generation system, which is significant and valuable for motivating the practical applications of hybrid power technology.

2. System description

The NG fueled SOFC-HCCI engine hybrid power generation system consists of two main subsystems, which are Pre-reforming-SOFC and HCCI-engine, as shown in Fig. 1. Herein, we take NG as input fuel for an example. The reason for choosing HCCI-engine is that the fuel of engine, which is in fact a lean fuel, directly comes from SOFC anode off-gas. As for the lean fuel, the best method to make the fuel burning in the engine is using the technology of homogeneous charge compression ignition (HCCI) which synergistically combines spark ignition (for gasoline) and compression ignition (for diesel) [26]. In the Pre-reforming-SOFC subsystem, the reformer first converts the preheated methane (the main composition of NG whose standard composition: 85% CH_4, 7% C_2H_6, 2% C_3H_8, 5% CO_2 and 1% N_2) into CO and H_2 as anode fuel of SOFC. The SOFC consumes the anode fuel and oxygen by electrochemical reaction to generate electricity. Then, the SOFC anode off-gas (main compositions: CO, CO_2, H_2, N_2, and H_2O) and cathode off-gas (air) after preheating pristine NG fuel enter into the downstream HCCI-engine subsystem as the fuel of the engine. In the HCCI-engine subsystem, the SOFC anode and cathode off-gas sequentially go through the processes of compression, combustion, and expansion stroke for additional power generation. The engine off-gas, which generally has a high temperature, is used to sequentially provide the thermal source for driving the pre-reforming reaction and heat the water into steam as the reactant of the pre-reforming reaction.

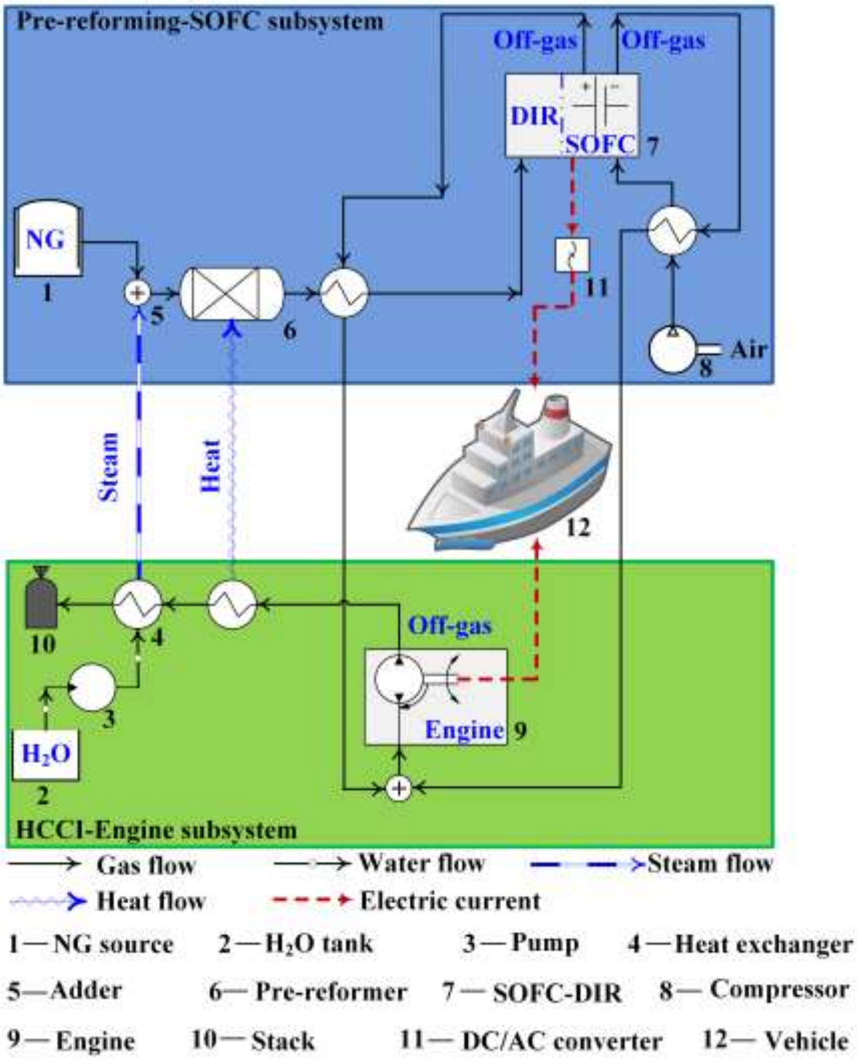

Fig. 1. The layout of the proposed NG fueled SOFC-HCCI engine hybrid power generation system

3. Steady-state thermodynamic modelling of the hybrid system

3.1. Model assumptions

The following assumptions are made for simplifying the system model.

1) The system is in a steady-state operation.
2) The NG source is desulfurized.
3) Pressure drops in the hybrid system are neglected. That's because that the pressure drops of the main components in the system were reported to be small [30-32].
4) The modeling of SOFC-DIR fully considered the reforming and the electrochemical reactions. The gas fuel after the reforming reaction equilibrium is the input fuel of the subsequent electrochemical reaction. The local isothermal model is applied to fuel cell for calculating electrochemical balance based on the constant cell temperature [33].
5) The hydrocarbon component in the NG is completely converted into H_2 in the SOFC-DIR due to the high temperature. The necessary heat required for the internal reforming reaction is taken from the electrochemical reaction in the SOFC.
6) The reforming and water gas shift (WGS) reactions in the system occur at the equilibrium temperature [34].
7) The system is well thermally insulated and the heat loss is negligible from the equipments (heat exchangers and reactors including the reformer, WGS, and MHR) to the environment.

3.2. Modelling methane reforming process

In the Pre-reformer and SOFC-DIR, the reforming reactions converting CH_4 into H_2 can be described in the following Eqs. (1) and (2), which represent the methane reforming and WGS reactions, respectively.

$$CH_4 + H_2O \rightarrow CO + 3H_2 \quad \Delta H = 206\ \mathrm{kJ/mol} \tag{1}$$

$$CO + H_2O \rightarrow CO_2 + H_2 \quad \Delta H = -41\ \mathrm{kJ/mol} \tag{2}$$

For the reforming reactions, the components of the reaction products (gas mixture) and their concentrations closely depend on the reaction equilibrium constant *K*, which is the function of reaction temperature only. Accordingly, the mathematical relationship between components and reaction temperature can be expressed in Eq. (3) [35, 36].

$$\begin{aligned} K_{reform} &= \frac{p_{CO} \cdot p_{H_2}^3}{p_{CH_4} \cdot p_{H_2O}} = f\left(T_{reform}\right) \\ &= -2.63121\times10^{-11}\cdot T^4 + 1.24065\times10^{-7}\cdot T^3 - 2.25232\times10^{-4}\cdot T^2 + 0.195028\cdot T - 66.1395 \quad \text{for reforming reaction} \\ K_{WGS} &= \frac{p_{CO_2} \cdot p_{H_2}}{p_{CO} \cdot p_{H_2O}} = f\left(T_{WGS}\right) \\ &= 5.47301\times10^{-12}\cdot T^4 - 2.57479\times10^{-8}\cdot T^3 + 4.63742\times10^{-5}\cdot T^2 - 0.03915\cdot T + 13.2097 \quad \text{for WGS reaction} \end{aligned} \tag{3}$$

3.3. Modelling SOFC-DIR subsystem

Besides the methane reforming and WGS reactions, the electrochemical reaction between H_2 and O_2 also takes place in the SOFC-DIR, which can be expressed by Eq. (4). Herein, it should be noticed that only H_2 is assumed as the fuel for electrochemical oxidation in the SOFC anode. Although the gas CO, the main mixture component after the methane reforming process, can also be electrochemically oxidized in the anode, its reaction rate is lower than that of the H_2 fuel. Moreover, the WGS reaction converting CO into H_2 always preferentially occurs in the presence of water.

$$H_2 + \frac{1}{2}O_2 \rightarrow H_2O(g) \quad \Delta H = -242\ \mathrm{kJ/mol} \tag{4}$$

In the SOFC-DIR model, the H_2 consumption is determined by the FC fuel utilization μ_{fuel} as written in Eq. (5), among which $\dot{m}_{H_2,in}$ is the molar flow sum of the effective components that can be converted into H_2 by reforming or WGS reactions.

$$\mu_{\mathrm{fuel}} = \frac{\dot{m}_{H_2,consumption}}{\dot{m}_{H_2,in}} \tag{5}$$

The overall mass balance of SOFC and the mass exchange between anode and cathode are described in Eqs. (6) and (7), respectively.

$$\phi_{a,in} + \phi_{c,in} - \phi_{a,out} - \phi_{c,out} = 0 \tag{6}$$

$$\phi_{c\rightarrow a} = \phi_{a,out} - \phi_{a,in} = M_{O_2} \cdot \frac{I}{4F} \tag{7}$$

The overall energy balance equation of SOFC is written as below.

$$\phi_{a,in} \cdot h_{a,in} + \phi_{c,in} \cdot h_{c,in} - \phi_{a,out} \cdot h_{a,out} - \phi_{c,out} \cdot h_{c,out} = P_{DC} + Q_{loss} \tag{8}$$

The relationship between anode mass flow $\phi_{a,in}$ and FC power output P_{FC} can be described in the following equation.

$$\phi_{a,in} \cdot \mu_{fuel} \cdot \eta_{fuel} \cdot LHV_{fuel} = \frac{P_{FC}}{\eta_{DC/AC}} = P_{DC} = A_{cell} \cdot J \cdot U_{ir} \tag{9}$$

Equation (10) gives the expression of current density J. Herein, $y_{a,in,i}$ stands for the concentration of the effective components involved with H_2 during the reforming and electrochemical reactions.

$$J = \frac{I}{A_{cell}} = \frac{\mu_{fuel}}{A_{cell}} \cdot \frac{\phi_{a,in}}{M_a} \cdot \frac{\sum_{i}^{n} y_{a,in,i}}{2F} \tag{10}$$

Through the combination of Eqs. (9) and (10), the FC power output P_{FC} can be expressed in the following function $f(\mu_{fuel})$ of fuel utilization μ_{fuel}.

$$P_{FC} = \eta_{DC/AC} \cdot I \cdot U_{ir} = \mu_{fuel} \cdot \frac{\phi_{a,in}}{M_a} \cdot \frac{\sum_i^n y_{a,in,i}}{2F} \cdot \eta_{DC/AC} \cdot U_{ir} \tag{11}$$

In Eq. (11), the irreversible cell voltage U_{ir} mainly depends on cell equilibrium conditions (cell pressure p_{Cell} and temperature T_{cell}), fuel compositions and current density. The corresponding relationship is written in Eq. (12), among which the overvoltage caused by the polarization is written in $U_{loss} = I \cdot R_{eq}$ with the assumption that the polarization overvoltage can be estimated by Ohm's law. The equivalent resistance R_{eq} is calculated and determined under the design conditions of cell voltage U_{ir} and current density J at the initial stage.

$$U_{ir} = E_T^0 + \frac{R_g \cdot T_{cell}}{2F} \cdot \ln\left[\left(\frac{y_{c,O_2}^{1/2} \cdot y_{a,H_2}}{y_{a,H_2O}}\right) \cdot p_{cell}^{1/2}\right] - I \cdot R_{eq} \tag{12}$$

The energy conversion efficiency of SOFC can be evaluated by the following expression:

$$\eta_{FC} = \frac{P_{FC}}{\phi_{NG} \cdot LHV_{NG}} \tag{13}$$

3.4. Modelling HCCI-engine subsystem

The thermodynamic cycle of the HCCI engine is generally an Otto-cycle, which can be described into the sequential processes of compression, combustion, expansion stroke and exhaust blow-down, as illustrated in Fig. 2. In our model, the compression and expansion strokes are assumed to be without gas exchange. During the engine working process, the SOFC anode off-gas and oxygen are first mixed to form a homogeneous mixture as the intake fuel, which is compressed for high-efficiency combustion. An isentropic model with the isentropic efficiency of 0.75 is usually applied to model the compression process. It was reported that the optimal compression ratio is about 4.4 for the micro gas turbine to achieve the maximum electrical power [26]. Therefore, the compression ratio in this work is also set as 4.4.

In the second stroke, the combustion process is typically isochoric due to a very fast volumetric combustion [37]. Then, the expansion stroke is considered as an isentropic process for external work. Finally, the exhaust blow-down to atmospheric pressure makes the Otto-cycle back to the thermodynamic state.

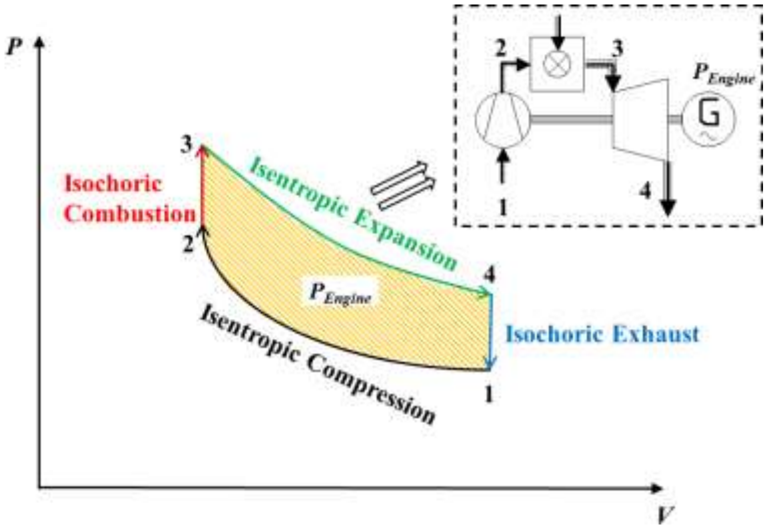

Fig. 2. The *P*-*V* diagram of the Otto-cycle and the corresponding schematic diagram for HCCI-engine working process

The energy balance equations for the components compressor and turbine are written in the following:

$$P_{Comp} \cdot \eta_{ISC} \cdot \eta_{MEC} = \phi \cdot (h_{out} - h_{in}) \tag{14}$$

$$P_{Turb} \cdot \eta_{IST} \cdot \eta_{MET} = \phi \cdot (h_{out} - h_{in}) \tag{15}$$

The energy equation over the combustor can be described in Eq. (16).

$$\phi_{fu} \cdot h_{fu} + \phi_{ox} \cdot h_{ox} = \phi_{as} \cdot h_{as} + \phi_{exh} \cdot h_{exh} \tag{16}$$

The relationship between reaction enthalpy and mass flux during the combustion process can be expressed by Eq. (17).

$$\Delta H_{comb} = \phi_{exh} \cdot h_{exh} - \phi_{n-rec} \cdot h_{n-rec} \tag{17}$$

Through the Otto-cycle, the HCCI engine generates a certain amount of power. The net power output P_{Engine} can be calculated as the work subtraction between expansion and compression strokes, as listed in Eq. (18). In other words, the value of

P_{Engine} is equivalent to the enclosed area of the *P-V* diagram in Fig. 2.

$$P_{Engine} = \phi \cdot \left[\left(h_3 - h_4 \right) - \left(h_2 - h_1 \right) \right] \tag{18}$$

The energy conversion efficiency of HCCI-engine hybrid system can be evaluated by Eq. (19).

$$\eta_{Engine} = \frac{P_{Engine}}{\phi_{fuel} \cdot LHV_{fuel}} \tag{19}$$

3.5. Computational details

In the present study, Cycle-Tempo software developed by Delft University of Technology (TU Delft) [38] is used to perform thermodynamic modeling and exergy analysis for optimizing the SOFC-HCCI engine hybrid system. The software is an elaborative simulation tool for thermodynamic modeling, which has been successfully applied to the energy system optimization and been proven to be a feasible and reliable simulator for the steady-state modeling [39-41]. The computational model of the proposed NG fueled SOFC-HCCI engine hybrid system is established and demonstrated in Fig. 3.

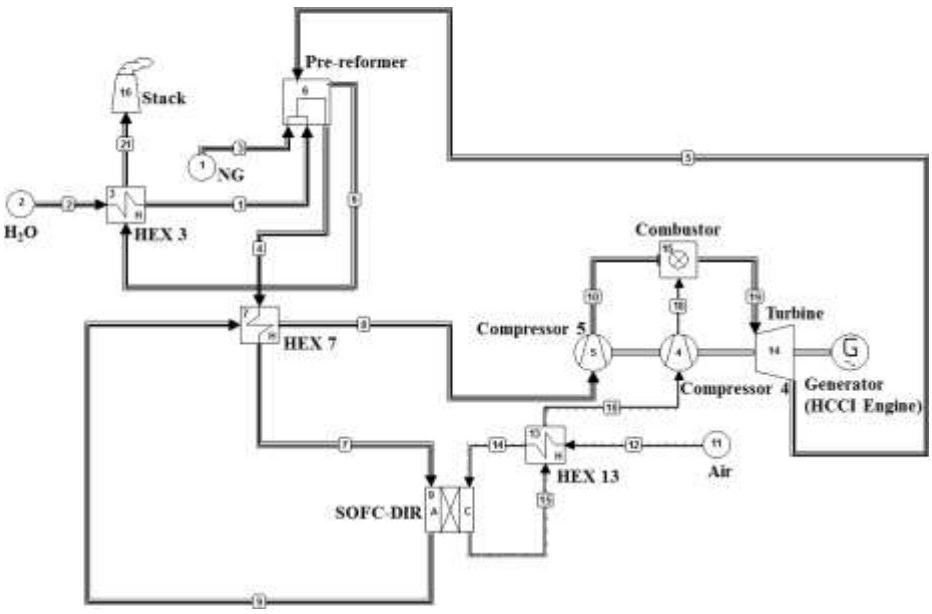

Fig. 3. The computational model of the proposed NG fueled SOFC-HCCI engine hybrid system

In the FC module, the counter flow between fuel and air is adopted. During the calculations, the acceptable relative error for the iteration operation is set as 1.0×10^{-4}. In addition, some important parameters used in the hybrid system modeling are summarized and listed in Table 1.

Table 1 Values of some important parameters used in the model of the hybrid system.

Parameter	Value
Operating pressure of the SOFC, p_{SOFC} (bar)	1.013
Equilibrium pressure of the DIR reaction, p_{reform} (bar)	1.013
DC/AC conversion efficiency, $\eta_{DC/AC}$	0.96
Cell voltage of SOFC, $U_{ir,SOFC}$ (V)	0.75
Isentropic efficiency of compressor, η_{ISC}	0.75
Mechanical efficiency of compressor, η_{MEC}	0.90
Isentropic efficiency of turbine, η_{IST}	0.80
Mechanical efficiency of turbine, η_{MET}	0.90
Generator efficiency, η_{GEN}	0.90

The overall energy conversion efficiency of the SOFC-HCCI engine hybrid power generation system can be calculated by Eq. (20).

$$\eta_{EN} = \frac{P_{FC} + P_{Engine}}{\phi_{fuel} \cdot LHV_{fuel}} \tag{20}$$

3.6. Model verification

As the proposed system is new, no relevant experimental data are available. In view of steady-state modeling in this paper, the verification of the SOFC-HCCI engine hybrid system model is performed by checking the model's energy balance.

Fig. 4 displays the energy input and output of the hybrid system. In our case, the energy input into the hybrid system includes NG, air, and water sources, while the energy going out of the system has stack gas besides the SOFC and engine power output.

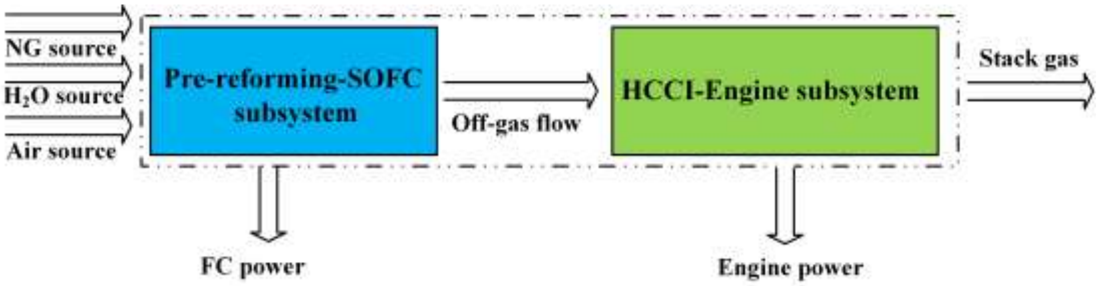

Fig. 4. The energy input and output of the NG fueled SOFC-HCCI engine hybrid system.

Herein, we randomly chose an operating point of NG mass flux $\phi_{NG} = 0.05$ kg/s to check the balance between input and output energy for verification. Table 2 lists the simulation results of gas compositions, input and output energy for the hybrid system. The error is only 0.01 kW between the input and output energy in the computational model, indicating the accuracy of the model for the SOFC-HCCI engine hybrid system.

Table 2 The energy balance verification of the SOFC-HCCI engine hybrid system.

Components			Energy (kW)	Total energy (kW)	Error (kW)
Input	NG source	CH_4: 85%, C_2H_6: 7%, C_3H_8: 2%, CO_2: 5%, N_2: 1%	181.63	2623.83	0.01
	Air source	N_2: 77.29%, O_2: 20.75%, CO_2: 0.03%, H_2O: 1.01%, Ar: 0.92%	456.26		
	H_2O source		1985.94		
Output	Output power	SOFC power	650.72	-2623.82	
		HCCI Engine power	510.39		
	Stack gas	N_2: 73.31%, O_2: 16.97%, CO_2: 1.39%, H_2O: 7.47%, Ar: 0.87%	-3784.93		

4. Results and discussion

4.1. Parametric analysis

As shown in Fig. 1, the NG-fueled SOFC-HCCI engine hybrid system contains three key components: pre-reformer, SOFC and HCCI engine. The operating parameters of each component easily affect other components' working conditions and thus determine the hybrid system's overall performance. For example, the SOFC fuel utilization ratio has a significant impact on the anode off-gas composition, and thus affects the combustion process of off-gas and oxygen in the HCCI engine. Actually, the changes in the FC off-gas composition and the engine combustion reaction indicate the variations of FC and engine power generation. In the present study, the influences of the following operating parameters on the overall performance of the hybrid system are investigated for further optimization, including the steam-to-carbon (S/C) ratio, pre-reforming temperature $T_{Pre\text{-}re}$, SOFC fuel utilization ratio μ_{FC} and operating temperature T_{FC}.

Fig. 5 shows the overall performance of the SOFC-HCCI engine hybrid system under different S/C ratios (2.0, 2.2, 2.5, 2.8 and 3.0). The other operating parameters for the hybrid system are set as Φ_{NG}=0.022 kg/s, $T_{Pre\text{-}re}$=540 ℃, T_{FC}=800 ℃ and μ_{FC}=0.5. It is found that the net electrical efficiency of the hybrid system decreases with the S/C ratio, which is mainly attributed to the reduction in the HCCI engine power generation. Actually, the SOFC power remains almost unchanged when the S/C ratio increases from 2.0 to 3.0. Although more CH_4 is converted into H_2 and CO by pre-reforming reaction at 540 ℃ under higher S/C ratio in the ex-reformer (Fig. 5b), the high SOFC temperature up to 800 ℃ makes SOFC an internal-reformer to almost completely convert the remaining CH_4 into H_2. The complete conversion of CH_4 component of NG source by the combination of ex- and internal-reforming reactions accounts for almost the same SOFC power generation. However, a higher S/C ratio easily results in smaller CO and H_2 compositions exhausted from the SOFC anode, as shown in Fig. 5b. The sum ratio of CO and H_2 in the anode off-gas reduces from 36.31% to 29.93% with an increase of S/C ratio from 2.0 to 3.0. In the SOFC-HCCI engine hybrid system, the anode off-gas is used as the engine fuel.

Therefore, the reduction in the CO and H_2 effective compositions inevitably brings about the reduction in the engine power generation, accordingly lowering the net electrical efficiency of the hybrid system. In order to avoid the carbon formation and deposition in the SOFC, keeping the S/C ratio more than 2.5 is generally recommended [42]. Consequently, the optimal S/C ratio of 2.5 is chosen to achieve high efficiency and simultaneously prevent carbon deposition in the hybrid system.

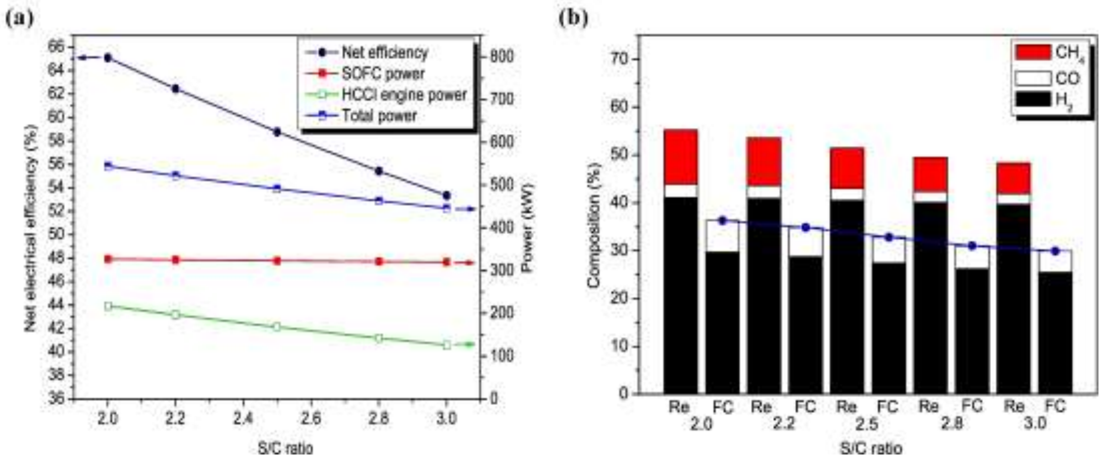

Fig. 5. The influence of S/C ratio on hybrid system performance. (a) Net electrical efficiency and power; (b) Main off-gas compositions of pre-reformer (Re) and SOFC (FC) components

Like the S/C ratio, the pre-reforming temperature of the ex-reformer has a similar impact on the electrical efficiency. The efficiency of the SOFC-HCCI engine hybrid system decreases with an increase of the pre-reforming temperature. Fig. 6 shows the hybrid system performance under different pre-reforming temperatures at Φ_{NG}=0.022 kg/s, S/C=2.5, T_{FC}=800 ℃ and μ_{FC}=0.5. On the one hand, the pre-reforming temperature shows little influence on the SOFC power generation since SOFC can act as an internal-reformer to almost completely convert the remaining CH_4 into H_2 at T_{FC}=800 ℃. On the other hand, the HCCI engine gross power, fuel and air compression work increase (shown in Fig. 6a) when the pre-reforming temperature is elevated from 540 to 600 ℃. This is because that the heat source for heating pre-reforming reaction comes from the exhaust gas of engine component by waste heat recovery in this case. The elevated pre-reforming temperature indicates more heat produced by the engine. Accordingly, more fuels are required for the engine to generate more power. Fig. 6b displays that the air mass flux input into the engine is increased from 1.24 to 2.05 kg/s when the pre-reforming temperature increases, which results in the significant increase of the air compression work. As a result, the net power generation of HCCI engine is reduced at an elevated pre-reforming temperature due to the remarkably increased fuels compression consumption. Therefore, the net electrical efficiency of the hybrid system was found to decrease with the elevation of the pre-reforming temperature. Considering that CH_4 steam reforming reaction generally takes place at a temperature higher than 500 ℃ [43,44], the optimal pre-reforming temperature is set as 540 ℃ for the SOFC-HCCI engine hybrid system to achieve high efficiency.

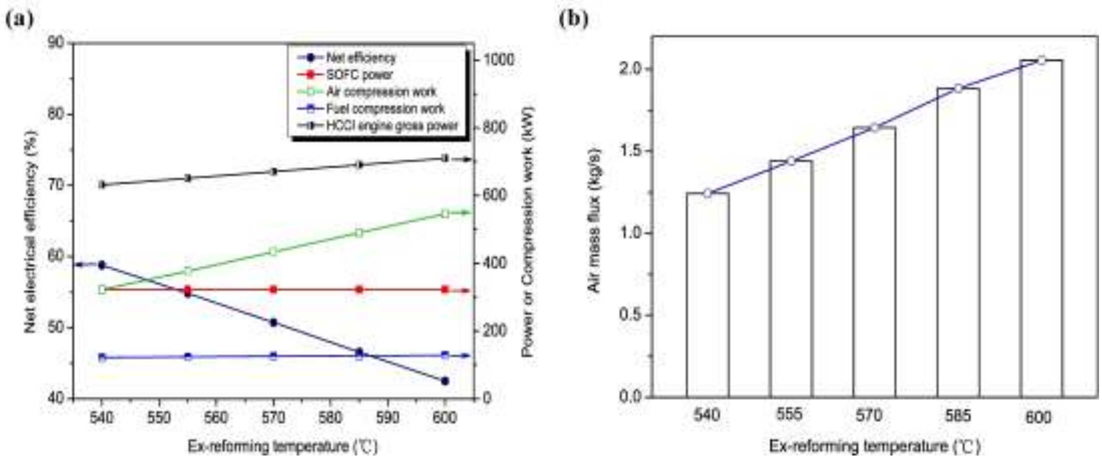

Fig. 6. The influence of pre-reforming temperature on hybrid system performance. (a) Net electrical efficiency, power and compression work; (b) Air mass flux

The influences of SOFC temperature and fuel utilization on the SOFC-HCCI engine hybrid system are further investigated. It is of importance to notice that the SOFC-HCCI engine hybrid system can be divided into three sub-regions according to the SOFC temperature and fuel utilization, as shown in Fig. 7. In the sub-region Ⅰ which has a relatively low temperature of no more than 600 ℃, the SOFC generally cannot work. Consequently, the sub-region Ⅰ represents the not working region of SOFC, which also indicates unavailability for the SOFC-HCCI engine hybrid system. At a temperature higher than 600 ℃, the region is separated into two sub-regions Ⅱ and Ⅲ determined by the relationship between SOFC temperature and fuel utilization. The blue dashed line including blue circle stands for the critical line determining whether the engine can generate power or not. In the sub-region Ⅲ which has a relatively high SOFC fuel utilization of more than 0.6, a majority of fuel is consumed in the SOFC so that the amount of CO and H_2 effective components from the SOFC anode off-gas are too low to support the power generation of engine. This is because the downstream engine uses the SOFC anode off-gas as fuel for electricity generation. Therefore, only SOFC works in the sub-region Ⅲ without HCCI Engine working. By contrast, both SOFC and HCCI engine work in the sub-region Ⅱ due to a relatively low fuel utilization. It was found that the limiting fuel utilization is about 0.59 for the hybrid system to simultaneously generate power by SOFC and engine. The corresponding net electrical efficiency of the hybrid system at the limiting fuel utilization is about 44%.

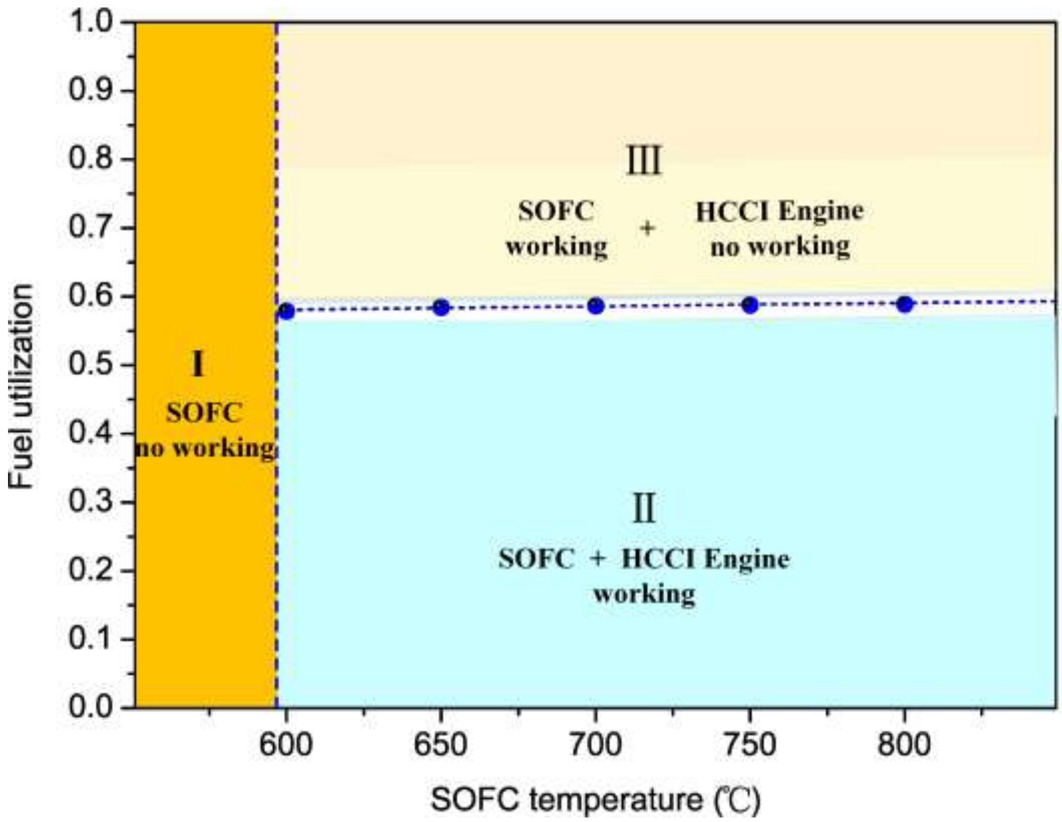

Fig. 7. Sub-regions of SOFC-HCCI engine hybrid system determined by SOFC temperature and fuel utilization: Ⅰ SOFC no working; Ⅱ SOFC and engine both working ; Ⅲ SOFC working and HCCI engine no working.

4.2. System performance and exergy analysis

The performance of the NG fueled SOFC-HCCI engine hybrid system is predicted under the fixed NG mass flux φ_{NG}=0.022 kg/s. According to the above-mentioned parametric analyses, the optimal operating parameters were found to be S/C ratio=2.5, T_{Pre-re}=540 ℃, and T_{FC}=800 ℃. The SOFC fuel utilization is mostly reported to be 0.85 for a single FC. However, it is very hard to maintain such a high fuel utilization for SOFC stack and system due to their complexity. Actually, it was reported that the real fuel utilization of SOFC system prototype is about 0.5 [45]. Thus, we also choose the real prototype fuel utilization μ_{FC}=0.5 to evaluate the system performance. Table 3 lists the NG-fueled SOFC-HCCI engine hybrid system performance. The hybrid system could generate 491.12 kW power when consuming 0.022 kg/s of NG as the input fuel. The corresponding NG fuel energy is calculated to be 835.98 kW (the LHV value). The total power consists of two parts, SOFC and HCCI engine, which output 323.11 and 168.01 kW, respectively. Actually, the expansion stroke of burning gas after the combustion reaction can generate 632.19 kW gross power. However, 445.51 kW of compression work is needed before the combustion process in the HCCI engine. Based on the Otto cycle shown in Fig. 2, the HCCI engine could generate the net power P_{Engine}=168.01 kW. According to Eq. (16), the net electrical efficiency and exergy efficiency are 58.75% and 56.68%, respectively. In this case, the energy conversion efficiency of individual SOFC and HCCI engine is approximately 39% and 34%, respectively. The calculated efficiency of the SOFC-HCCI engine hybrid system in our study is comparable to that of the previously reported SOFC-HCCI engine hybrid system (59.5%) [26] as shown in Fig. 8. We also compare the energy conversion efficiency of the proposed hybrid system with other fuel cell power systems, such as Reformer-PEMFC (R-PEMFC) [46], SOFC-CLHP [47], simple SOFC and SOFC-GT [26,48]. It can be seen that the SOFC-HCCI engine hybrid system has a higher efficiency than these FC power systems. Especially, the SOFC-HCCI engine hybrid system has a slightly higher efficiency than the SOFC-GT hybrid system, suggesting that the method of using SOFC anode off-gas as HCCI engine fuel is feasible and effective to improve the energy conversion efficiency of FC power systems.

Table 3. The calculated power generation, energy and exergy efficiency of the SOFC-HCCI engine hybrid system at ϕ_{NG}=0.022 kg/s.

	Input energy (kW)	Total power generation (kW)				Efficiency	
			HCCI-engine				
	NG fuel	SOFC	Net power	Gross power	Compression work	Energy	Exergy
Value	835.98	323.11	168.01	632.19	445.51	58.75%	56.68%

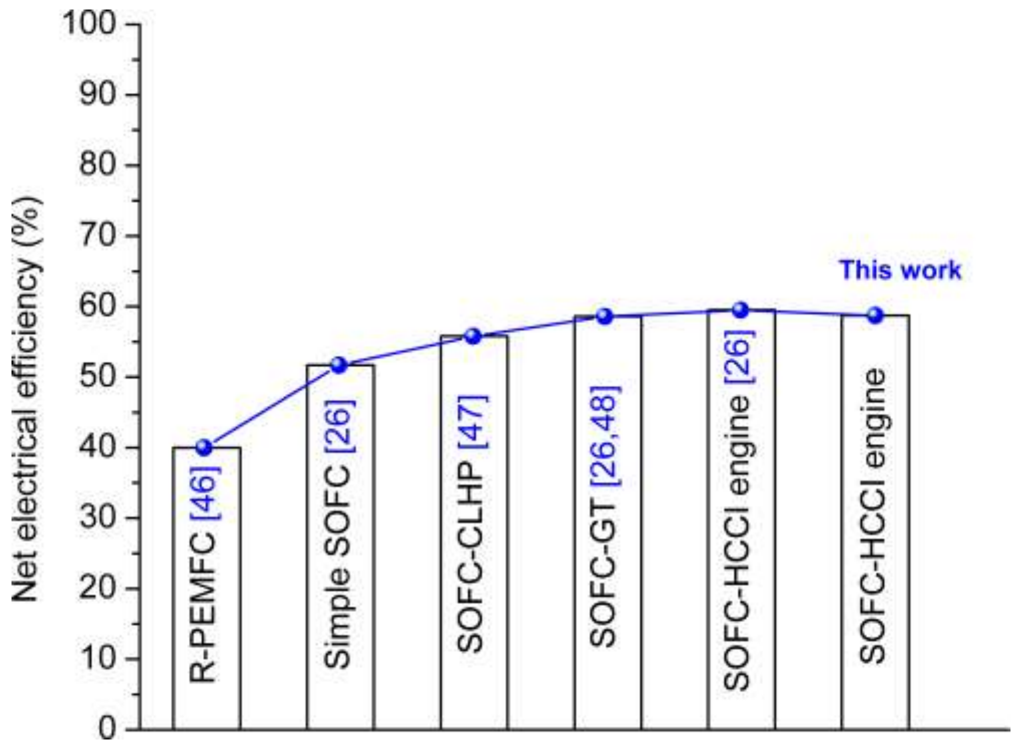

Fig. 8. The comparison of energy conversion efficiency among different fuel cell power generation systems [26, 46-48].

The exergy analysis in the SOFC-HCCI engine hybrid system is further performed to identify which component of the system dominates the energy irreversibility of the whole system, thus providing approaches to optimize the system performance. Here, it should be noticed that the exergy analysis in this paper is carried out under the same environment condition p=1.013 bar and T=15 ℃. In the hybrid system, the exergy efficiency can be calculated by the following equation:

$$\xi_{EX} = \frac{Ex_{SOFC} + Ex_{Engine}}{Ex_{NG}} \quad (21)$$

The exergy efficiency of the SOFC-HCCI engine hybrid system under the optimal operating conditions is calculated to be 56.68%, as listed in Table 3. The corresponding exergy flow in the hybrid system is further investigated and shown in Fig. 9. In the hybrid system, the exergy flow starts from the NG fuel source with $Ex_{NG} = 866.49$ kW as 100% exergy input, and then sequentially enters into ex-reforming, SOFC, and HCCI engine subsystems. It was found that a total exergy destruction of 43.32% appears in the hybrid system, among which the ex-reforming, SOFC and HCCI engine subsystems contribute to 2.91%, 7.76%, and 18.86%, respectively. Besides the three main parts, the exhaust gas out of the Engine also delivers a large portion of exergy destruction (13.79%). It can be seen that the HCCI engine subsystem has the largest exergy destruction and the exhaust gas has the second largest one. These two parts contribute to approximately 75% exergy destruction of the whole hybrid system, indicating the HCCI engine subsystem dominates the exergy destruction. Fig. 10 presents the exergy loss of the components and the corresponding ratio to the total exergy loss in the hybrid system. The relative exergy loss of the engine subsystem reaches up to 43.54%, which is the largest. In the HCCI engine subsystem, the exergy loss occurs in the components of compressors, combustor, turbine and generator. The compressors with the relative exergy loss of about 24% take up more than half of the exergy destruction of the engine subsystem. The relative exergy loss of air compression is calculated to be 8.30%, which is nearly four times as large as that of the fuel compression. The other components of the engine subsystem contribute to the relative exergy loss of about 19%. Besides, the exhaust gas out of the engine with the relative exergy loss of 31.83% also plays a significant role in the system exergy destruction. Actually, the exhaust gas, whose temperature is approximately 65 ℃, contains a certain amount of waste heat. If this part of waste heat could be effectively recycled with the aim of improving the thermal efficiency, the overall efficiency of the hybrid system will be significantly improved. As mentioned before in Table 3, the output power of the SOFC and HCCI engine are

323.11 and 168.01 kW, respectively. The ratio of engine to total power is about 0.34, which is thought to be relatively low in the hybrid system. That's to say, the engine power ratio is generally low in the proposed SOFC-HCCI engine hybrid system. Nevertheless, the engine takes up a major part of exergy destruction. Therefore, it could be concluded that the HCCI engine has a small contribution to the power generation but exhibits a large exergy destruction in the hybrid system.

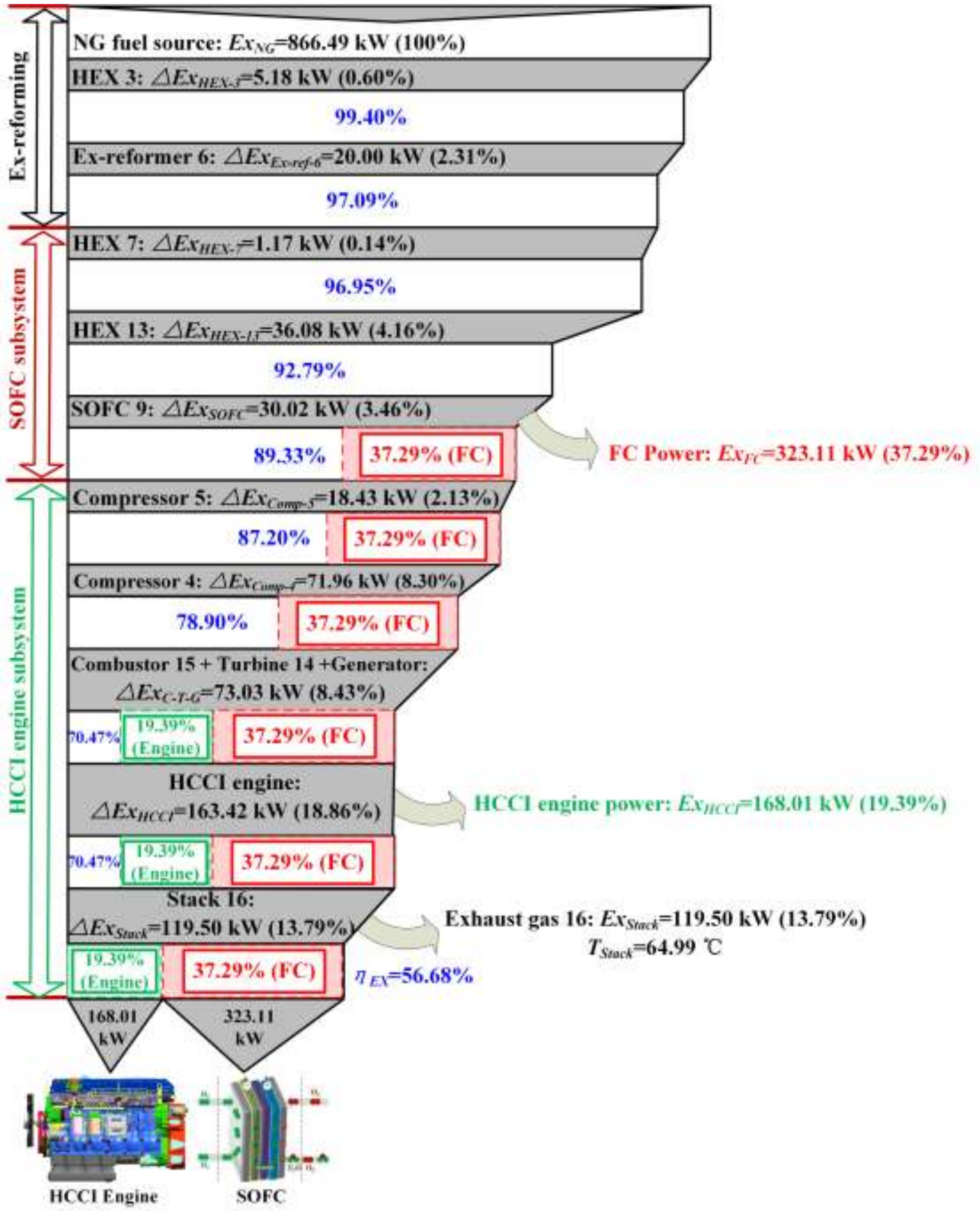

Fig. 9. Exergy flow diagram of the SOFC-HCCI engine hybrid system.

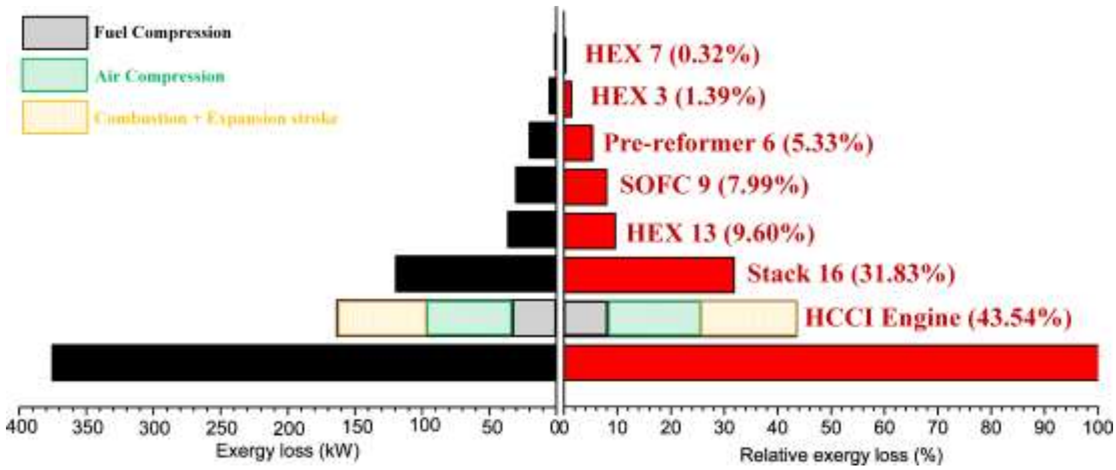

Fig. 10. Absolute and relative exergy loss of the main components in the SOFC-HCCI engine hybrid system.

4.3. Performance optimization and operating strategy

On the basis of the above-mentioned analyses, two features of the SOFC-HCCI engine hybrid system are observed. One is the relatively low engine power ratio, and the other is neglecting the waste heat recovery of the exhaust gas (T=64.99 ℃). The potential approach for improving the efficiency is to effectively utilize the waste heat of the exhaust gas to increase the engine power ratio. In this work, a small amount of H_2 addition into SOFC anode off-gas is considered as the engine input fuel to increase the engine power output. Herein, besides no H_2 addition for Case 1 (shown in Fig. 1), additional two cases for supplying H_2 to the engine are investigated, which are H_2 storage tank (HyT) for Case 2 and metal hydride reaction (MHR) for Case 3.

For Case 2, the H_2 addition is provided by physical hydrogen storage. No thermal effect occurs between HyT and engine. The role of H_2 addition by HyT is to increase the engine power ratio only, thus affecting the system overall efficiency. By contrast, the MHR for H_2 addition in Case 3 is completely a chemical hydrogen storage. The working principle is that metal hydrides can reversibly absorb and desorb H_2 at certain temperatures. That's to say, it requires heating of the MHR to drive the hydrogen desorption reaction of metal hydrides, thus supplying H_2 addition for the engine. Actually, the exhaust gas could generate the heat with the temperature of no more than 70 ℃, which is sufficient to drive the hydrogen desorption reaction of AB_5-type metal hydrides. The reversible hydrogen absorption/desorption reactions of

AB_5-type $LaNi_{4.3}Al_{0.7}$ with a reaction enthalpy of 29.2 kJ/mol H_2 can be described by Eq. (22) [49]. Therefore, recycling the waste heat of the exhaust gas for H_2 addition by MHR in Case 3 not only increases the engine power ratio but also enhances the thermal efficiency, and thus improves the system overall efficiency. The schematic diagram of the modified SOFC-HCCI engine coupled with MHR for H_2 addition (Case 3) is demonstrated in Fig. 11. The MHR reaction heat comes from the exhaust gas out from the HCCI engine subsystem for waste heat recovery.

$$LaNi_{4.3}Al_{0.7} + 3H_2 \underset{60\sim70^{\circ}C}{\overset{RT}{\longleftrightarrow}} LaNi_{4.3}Al_{0.7}H_6 + 29.2\ \text{kJ/mol}\ H_2 \qquad (22)$$

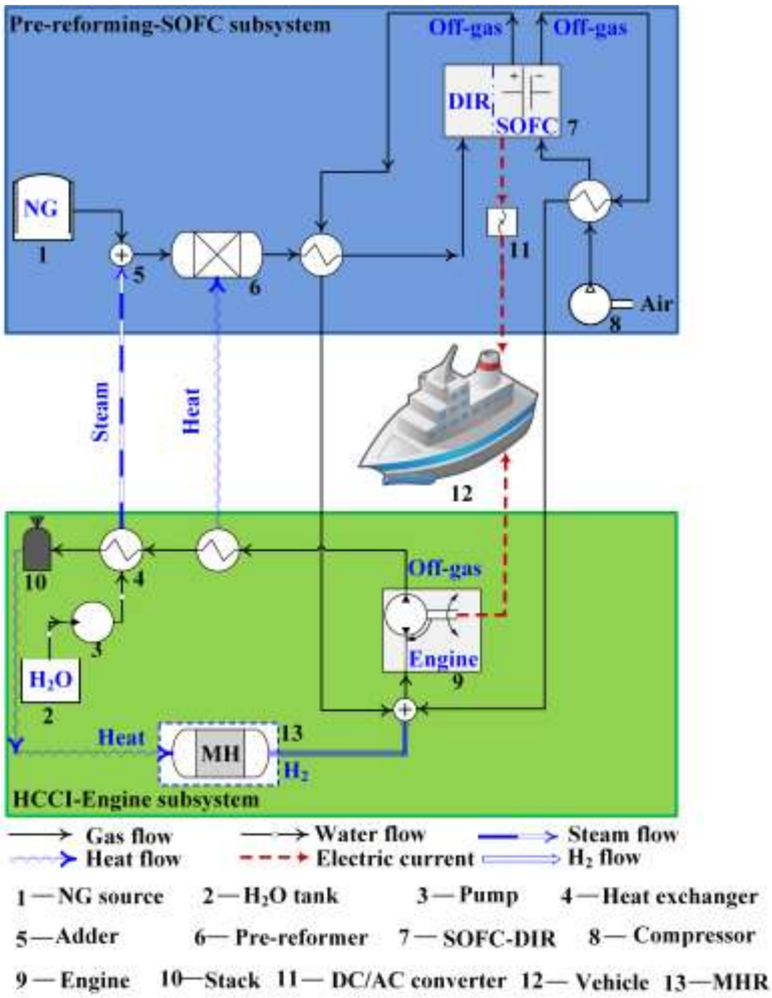

Fig. 11. The layout of the modified SOFC-HCCI Engine hybrid power generation system coupled with MHR for additional H_2 supply

The overall efficiency of the hybrid system under the three cases, which are Case 1 without H_2 addition, Case 2 with HyT and Case 3 with MHR for H_2 addition, is first compared under the same conditions. Fig. 12 displays the comparison of the overall efficiency between these three cases with different amounts of H_2 addition. It was found that more H_2 addition results in higher efficiency of the hybrid system. When the amount of H_2 addition is 5%, the efficiency of these three cases is 58.75%, 60.46%, and 65.98%, respectively, which is improved by 1.7% and 7.2 % for HyT and MHR to achieve H_2 addition. When further increasing the H_2 addition, the hybrid system coupled with MHR (Case 3) presents a much higher efficiency than the other two cases. This is because the thermal efficiency is taken into consideration in Case 3 due to the waste heat recovery of engine exhaust gas. Therefore, the method of MHR for H_2 addition by chemisorption is regarded as an efficient approach for improving the efficiency of the hybrid system. The detailed explanation is discussed in the following sections.

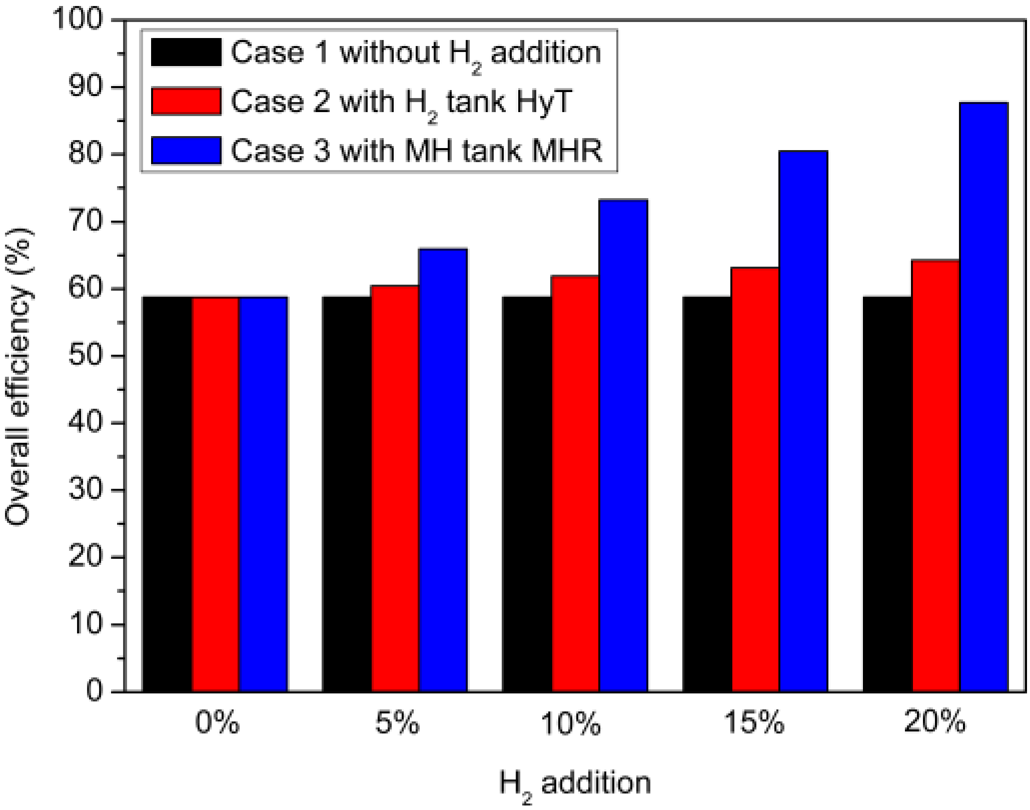

Fig. 12. The comparison of overall efficiency between the three cases with different amounts of H_2 addition.

Figs. 13a and 13b show the overall performance of Case 2 and Case 3 after H_2 addition by HyT and MHR, respectively. It can be clearly seen from Fig. 13a that the overall efficiency calculated by Eq. (23) increases with the amount of H_2 addition.

When the amount of H_2 addition changes from 5% to 20%, the efficiency of the hybrid system coupled with HyT for H_2 addition increases by 1.7% to 5.5%. This is because the addition of H_2 as fuel contributes to a significant increase in the HCCI engine power. Considering few impacts of H_2 addition on the SOFC power, the total power of the hybrid system is remarkably increased. Although the additional H_2 source LHV is input and also increases with the H_2 addition in a linear pattern, the conversion efficiency of additional H_2 source is found to be higher than that of the pristine NG source. Therefore, it can be concluded that the addition of H_2 into SOFC anode off-gas as fresh fuel for the engine is conducive to the improvement of system overall efficiency.

$$\eta_{EN} = \frac{P_{FC} + P_{Engine}}{\phi_{NG} \cdot LHV_{NG} + \phi_{H_2} \cdot LHV_{H_2}} \tag{23}$$

In the same way, the overall efficiency of the SOFC-HCCI engine hybrid system coupled with MHR for H_2 addition increases with the amount of H_2 addition. By comparison, the improvement degree of Case 3 is much higher than that of Case 2. Up to 7.2% ~ 28.2% increase appears in Case 3 when the amount of H_2 addition increases from 5% to 20%. The comparison illustrates that the method of MHR for H_2 addition is more effective and efficient than that of HyT for NG-fueled SOFC-HCCI engine hybrid system. The high efficiency is ascribed to the waste heat recovery of the exhaust gas to achieve the hydrogen addition from MHR. On the one hand, the utilization of waste heat helps to improve thermal efficiency. On the other hand, no additional H_2 source is needed for the MHR supplying. As seen from the inset in Fig. 13b, the required heat for MHR to desorb 20% of H_2 is calculated to be approximately 38 kW, which can be completely covered by the exhaust gas energy (119.50 kW). It strongly suggests that the waste heat of the exhaust gas is enough to drive AB_5-type metal hydrides supplying up to 20% H_2 for the engine. In addition, the addition of H_2 plays an important role in the regulation of the power distribution between the SOFC and the engine for the SOFC-HCCI engine hybrid system. The H_2 addition of up to 20% by the MHR in Case 3 can result in the reduction of power ratio of SOFC to Engine from 1.92 to 0.79. When the amount of H_2 addition is 12.82%, the hybrid system exhibits half and half power for SOFC and HCCI engine components, both of which are 323 kW. In such a situation when taking thermal efficiency into consideration, the overall efficiency of the hybrid system coupled with MHR for both waste heat recovery and H_2 addition can reach up to 77.3%, higher than those of the SOFC-GT (70.6%) and SOFC-Engine (71.1%) hybrid systems coupled with HRSG (heat recovery steam generator) for waste heat recovery [26].

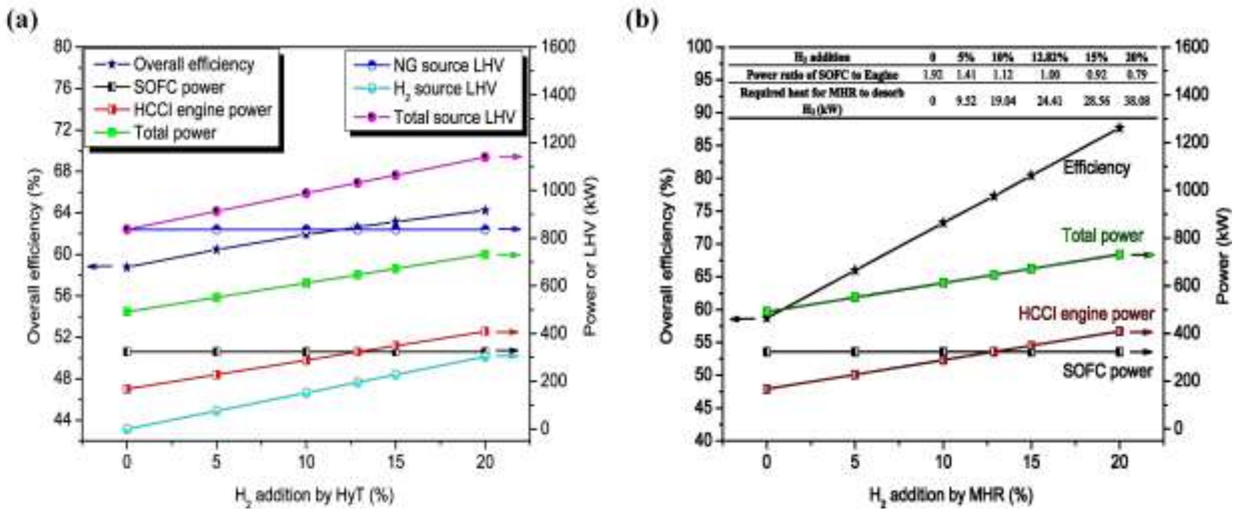

Fig. 13. System performance of the modified SOFC-HCCI engine hybrid system coupled with H_2 addition in different cases: (a) Case 2 H_2 tank (HyT); (b) Case 3 metal hydride reactor (MHR).

The afore-mentioned results demonstrate that the method of MHR for H_2 addition by waste heat recovery can significantly improve the overall efficiency of the SOFC-HCCI engine hybrid system. As described before, this method focuses on the HCCI engine subsystem and how to increase the engine power ratio and recycle the waste heat of the exhaust gas. Besides the HCCI engine subsystem, the SOFC subsystem is also an important component that affects the system efficiency. Actually, the actual fuel utilization of SOFC is a little low in practice, resulting in insufficiently high efficiency for the SOFC [50]. Therefore, H_2 recirculation for SOFC anode is considered to further improve the overall efficiency of the SOFC-HCCI engine hybrid system. Herein, we investigated the H_2 recirculation range of 0 to 50% for improving fuel utilization (the initial value is 0.5 in our work). Fig. 14 shows the effect of H_2 recirculation ratio on the system efficiency of the SOFC-HCCI engine hybrid system coupled with MHR for H_2 addition. It can be seen that the efficiency increases with an increase of the H_2 recirculation ratio. When the H_2 recirculation ratio is from 0 to 0.5, the efficiency increases from 77.30% to 79.54% accordingly. The increase in efficiency is mainly attributed to the increased SOFC output power caused by the higher fuel utilization. Therefore, it can be concluded that the method of H_2 recirculation for SOFC anode also helps to the improvement of the SOFC-HCCI engine hybrid system besides using waste heat recovery to drive MHR for H_2 addition. It is also noted that the proposed system is complex and it is crucial to carefully control the operating conditions in order to achieve the predicted efficiency.

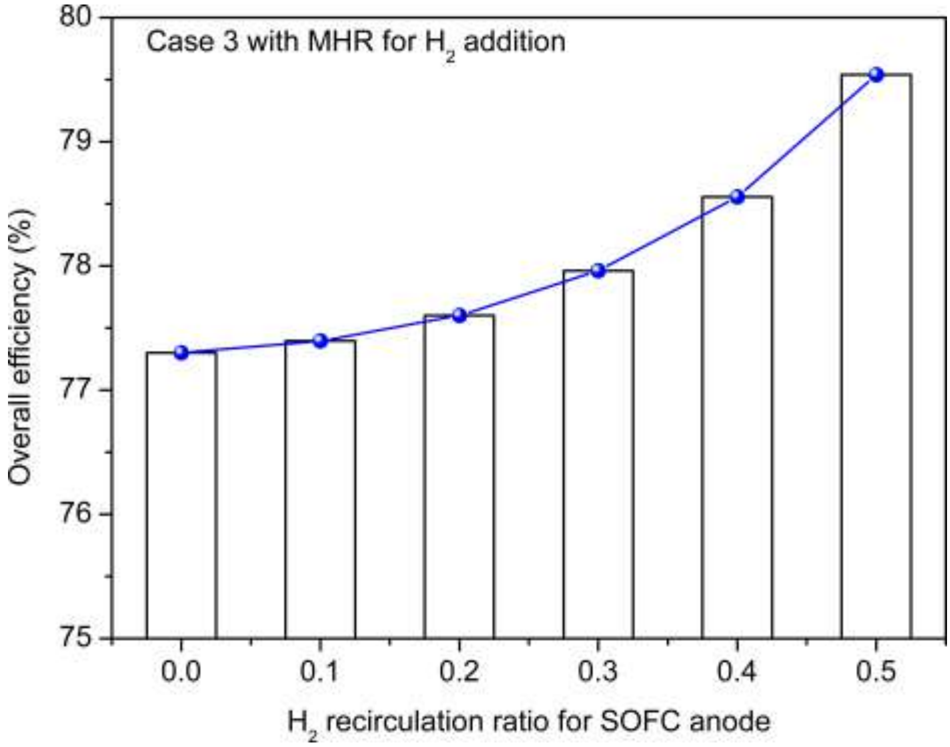

Fig. 14. Effect of H_2 recirculation ratio on the overall efficiency of the SOFC-HCCI engine hybrid system.

In the practical application, the hydrogen safety should be considered for the SOFC-HCCI engine hybrid system. The system discussed in this work mainly consists of SOFC, metal hydride reactor and HCCI engine subsystems. For the SOFC, the anode fuel is natural gas, indicating the SOFC is safe from the view of hydrogen safety. The metal hydride reactor is a kind of solid-state hydrogen storage, whose hydrogen plateau pressure is moderate (< 1 MPa for AB_5-type metal hydride) and far lower than that of compressed hydrogen storage (> 30 MPa). Therefore, compared with the compressed hydrogen storage, metal hydride solid-state hydrogen storage is much safer. The metal hydride reactor is also safe for H_2 addition due to its moderate plateau pressure and operating temperature (< 100 ℃). Although explosion of hydrogen-air mixture can easily occur at extremely high temperatures, many technical measures have been proposed to ensure the hydrogen safety of the engine, such as variable valve timing technology, backfire arrestor and so on. Actually, the HCNG (hydrogen and compressed natural gas) engine has been successfully developed and achieved the commercial applications in recent years. Only in the case of high loads at low speeds for the HCNG engine, the hydrogen explosion (also called combustion knock) may take place. However, this case is hard to occur in practice because this operating condition should be considered and avoided in the beginning of engine design. Besides, the content of H_2 addition into the engine is not high, only up to 20 vol.% in this work. In a word, the hydrogen safety of SOFC-HCCI engine hybrid system can be ensured in the practical application.

5. Conclusions

In summary, a novel SOFC-HCCI engine hybrid power generation system coupled with MHR for H_2 addition by waste heat recovery is proposed in the present study. A steady-state model of the hybrid system is established, and parametric and exergy analyses are performed and discussed for the performance optimization, achieving the corresponding operating strategy for the hybrid system. The conclusions are drawn as follows:

(1) The SOFC-HCCI engine hybrid power generation system exhibits a high net electrical efficiency up to 58.75%, which is also more efficient than the reported Reformer-PEMFC, simple SOFC, and SOFC-CLHP fuel cell systems. In addition, the hybrid system has comparable efficiency to the SOFC-GT hybrid system. The high energy conversion efficiency indicates that the method of using SOFC anode off-gas as HCCI engine fuel is feasible and effective to improve the FC system efficiency.

(2) In the hybrid system, the HCCI engine with a small contribution in the power

generation dominates the exergy destruction, which has the relative exergy loss of up to 43.54%. On the other hand, the SOFC component presents a larger power contribution and less exergy destruction.

(3) The hybrid system coupled with MHR for H_2 addition by waste heat recovery has a significantly improved overall efficiency compared to that with HyT for H_2 addition or without H_2 addition. Besides, the H_2 recirculation is also suggested for the SOFC anode off-gas to further increase the hybrid system efficiency by 2.24%.

(4) The SOFC-HCCI engine hybrid system is a promising energy conversion device due to high efficiency and fuel flexibility. The operation strategies of H_2 addition by metal hydride for HCCI engine and H_2 recirculation for SOFC are recommended for the hybrid system.

Acknowledgments

Z. Wu thanks the funding support from Hong Kong Scholar Program (XJ2017023) and the National Natural Science Foundation of China (21736008). P. Tan thanks the funding support from CAS Pioneer Hundred Talents Program. M. Ni thanks the funding support from The Hong Kong Polytechnic University (G-YBJN and G-YW2D), a fund from RISUD (1-ZVEA), and a grant (Project Number: PolyU 152214/17E) from Research Grant Council, University Grants Committee, Hong Kong SAR.

References

[1] Nowotny J, Dodson J, Fiechter S, Gur T, Kennedy B, Macyk W, et al. Towards global sustainability: Education on environmentally clean energy technologies. Renew Sustain Energy Rev 2018;81:2541–2551.

[2] Ni M, 2D thermal modeling of a solid oxide electrolyzer cell (SOEC) for syngas

production by H2O/CO2 co-electrolysis, International Journal of Hydrogen Energy 2012; 37(8): 6389-6399.

[3] Ni M, Leung MKH, Leung DYC, Energy and exergy analysis of hydrogen production by a proton exchange membrane (PEM) electrolyzer plant. Energy Conversion and Management 2008; 49(10): 2748-2756.

[4] Shan S, Zhou Z, Cen K. An innovative integrated system concept between oxy-fuel thermo-photovoltaic device and a Brayton-Rankine combined cycle and its preliminary thermodynamic analysis. Energy Convers Manage 2019;180:1139–1152.

[5] Damo UM, Ferrari ML, Turan A, Massardo AF. Solid oxide fuel cell hybrid system: A detailed review of an environmentally clean and efficient source of energy. Energy 2019;168:235–246.

[6] Überalla A, Otte R, Eilts P, Krahi J. A literature research about particle emissions from engines with direct gasoline injection and the potential to reduce these emissions. Fuel 2015;147:203–207.

[7] Liu H, Wang Z, Wang J, He X. Improvement of emission characteristics and thermal efficiency in diesel engines by fueling gasoline/diesel/PODEn blends. Energy 2016;97:105–112.

[8] Pedrozo VB, May I, Guan W, Zhao H. High efficiency ethanol-diesel dual-fuel combustion: A comparison against conventional diesel combustion from low to full engine load. Fuel 2018;230:440–451.

[9] Porpatham E, Ramesh A, Nagalingam B. Effect of hydrogen addition on the performance of a biogas fueled spark ignition engine. Int J Hydrogen Energy 2007;32:2057–2065.

[10] Bhasker JP, Porpatham E. Effects of compression ratio and hydrogen addition on lean combustion characteristics and emission formation in a Compressed Natural Gas fueled spark ignition engine. Fuel 2017;208:260–270.

[11] Bizon N, Thounthong P. Fuel economy using the global optimization of the Fuel Cell Hybrid Power Systems. Energy Convers Manage 2018;173:665–678.

[12] Sulaiman N, Hannan MA, Mohamed A, Ker PJ, Majlan EH, Wan Daud WR. Optimization of energy management system for fuel-cell hybrid electric vehicles:

Issues and recommendations. Appl Energy 2018;228:2061–2079.

[13] Song K, Chen H, Wen P, Zhang T, Zhang B, Zhang T. A comprehensive evaluation framework to evaluate energy management strategies of fuel cell electric vehicles. Electrochemica Acta 2018;292:960–973.

[14] Xu HR, Chen B, Tan P, Cai WZ, He W, Farrusseng D, et al. Modeling of all porous solid oxide fuel cells. Appl Energy 2018;219:105–113.

[15] Zhang HC, Kong W, Dong FF, Xu HR, Chen B, Ni M. Application of cascading thermoelectric generator and cooler for waste heat recovery from solid oxide fuel cells. Energy Convers Manage 2017;148:1382–1390.

[16] Taube M, Rippin DWT, Cresswell DL, Knecht W. A system of hydrogen-powered vehicles with liquid organic hydrides. Int J Hydrogen Energy 1983;8:213–225.

[17] McPhail SJ, Aarva A, Devianto H, Bove R, Moreno A. SOFC and MCFC: commonalities and opportunities for integrated research. Int. J. Hydrogen Energy 2011;36:10337–103435.

[18] Zhang X, Chan SH, Li G, Ho HK, Li J, Feng Z. A review of integration strategies for solid oxide fuel cells. J Power Sources 2010;195:685–702.

[19] Buonomano A, Calise F, d'Accadia MD, Palombo A, Vicidomini M. Hybrid solid oxide fuel cells-gas turbine systems for combined heat and power: A review. Appl Energy 2015;156:32–85.

[20] Cheddie DF. Thermo-economic optimization of an indirectly coupled solid oxide fuel cell/gas turbine hybrid power plant. Int J Hydrogen Energy 2011;36:1702–1709.

[21] Inui Y, Matsumae T, Koga H, Nishiura K. High performance SOFC/GT combined power generation system with CO_2 recovery by oxygen combustion method. Energy Convers Manage 2005;46:1837–1847.

[22] Kandepu R, Imsland L, Foss BA, Stiller C, Thorud B, Bolland O. Modeling and control of a SOFC-GT-based autonomous power system. Energy 2007;32:406–417.

[23] Zhang X, Su S, Chen J, Zhao Y, Brandon N. A new analytical approach to evaluate and optimize the performance of an irreversible solid oxide fuel cell-gas turbine hybrid system. Int J Hydrogen Energy 2011;36:15304–15312.

[24] Cheddie DF. Integration of a solid oxide fuel cell into a 10 MW gas turbine power plant. Energies 2010;3:754–769.

[25] Choi W, Kim J, Kim Y, Kim S, Oh S, Song HH. Experimental study of homogeneous charge compression ignition engine operation fueled by emulated solid oxide fuel cell anode off-gas. Appl Energy 2018;229:42–62.

[26] Park SH, Lee YD, Ahn KY. Performance analysis of an SOFC/HCCI engine hybrid system: system simulation and thermo-economic comparison. Int J Hydrogen Energy 2014;39:1799–1810.

[27] Kang S, Ahn KY. Dynamic modeling of solid oxide fuel cell and engine hybrid system for distributed power generation. Appl Energy 2017;195:1086–1099.

[28] Lee YD, Ahn KY, Morosuk T, Tsatsaronis G. Exergetic and exergoeconomic evaluation of an SOFC-Engine hybrid power generation system. Energy 2018;145:810–822.

[29] Dicks AL, Fellows RG, Mescal CM, Seymour C. A study of SOFC-PEM hybrid systems. J Power Sources 2000;86:501–506.

[30] Burbank W, Witmer D, Holcomb F. Model of a novel pressurized solid oxide fuel cell gas turbine hybrid engine. J Power Sources 2009;193:656–664.

[31] Wu Z, Yang FS, Zhang ZX, Bao ZW. Magnesium based metal hydride reactor incorporating helical coil heat exchanger: Simulation study and optimal design. Appl Energy 2014;130:712–722.

[32] Li Y, Ye S, Wang WG. Performance analysis of SOFC system based on natural gas autothermal reforming. CIESC Journal 2016;67:1557–1564.

[33] de Groot A. Advanced exergy analysis of high temperature fuel cell systems. Doctoral Thesis, The Energy Research Centre of the Netherlands, Petten, Netherlands, 2004.

[34] Ni M. Modeling and parametric simulations of solid oxide fuel cells with methane carbon dioxide reforming. Energy Conversion and Management 2013;70:116–129.

[35] Chan SH, Ho HK, Tian Y. Modelling of simple hybrid solid oxide fuel cell and gas turbine power plant. J Power Sources 2002;109:111–120.

[36] Massardo AF, Lubelli F. Internal reforming solid oxide fuel cell-gas turbine combined cycles (IRSOFC-GT). Part A. Cell model and cycle thermodynamic analysis. J Eng Gas Turbines Power 2000;122:27–35.

[37] Osborne RJ, Li G, Sapsford SM, Stokes J, Lake TH. Evaluation of HCCI for future gasoline powertrains. In: SAE 2003 world congress & exhibition 2003-01-0750 2003.

[38] van der Lee PEA, Terlaky T, Woudstra T. A new approach to optimizing energy systems. Comput Method Appl M 2001;190:5297–5310.

[39] Vera D, de Mena B, Jurado F, Schories G. Study of a downdraft gasifier and gas engine fueled with olive oil industry wastes. Appl Therm Eng 2013;51:119–129.

[40] Bagdanavicius A, Jenkins N. Exergy and exergoeconomic analysis of a compressed air energy storage combined with a district energy system. Energy Convers Manage 2014;77:432–440.

[41] Muhammad U, Imran M, Lee DH, Park BS. Design and experimental investigation of a 1 kW organic Rankine cycle system using R245fa as working fluid for low-grade waste heat recovery from steam. Energy Convers Manage 2015;103:1089–1100.

[42] Jørgensen SL, Nielsen PEH, Lehrmann P. Steam reforming of methane in a membrane reactor. Catal Today 1995;25:303–307.

[43] Matsumura Y, Nakamori T. Steam reforming of methane over nickel catalysts at low reaction temperature. Appl Catal A-Gen 2004;258:107–114.

[44] Lin YM, Liu SL, Chuang CH, Chu YT. Effect of incipient removal of hydrogen through palladium membrane on the conversion of methane steam reforming: Experimental and modeling. Catal Today 2003;82:127–139.

[45] Yang SQ. Simulation and analysis of system based on anode-supported SOFC. Doctoral Thesis, University of Chinese Academy of Sciences, Beijing, China, 2013.

[46] Marcoberardino GD, Roses L, Manzolini G. Technical assessment of a micro-cogeneration system based on polymer electrolyte membrane fuel cell and fluidized bed autothermal reformer. Appl Energy 2016;162:231–244.

[47] Aghaie M, Mehrpooya M, Pourfayaz F. Introducing an integrated chemical

looping hydrogen production, inherent carbon capture and solid oxide fuel cell biomass fueled power plant process configuration. Energy Convers Manage 2016;124:141–154.

[48] Akkaya AV, Sahin B, Erdem HH. An analysis of SOFC/GT CHP system based on exergetic performance criteria. Int J Hydrogen Energy 2008;33:2566–2577.

[49] Sharma VK, Kumar EA. Effect of measurement parameters on thermodynamic properties of La-based metal hydrides. Int J Hydrogen Energy 2014;39:5888–5898.

[50] Wu Z, Zhang ZX, Ni M. Modeling of a novel SOFC-PEMFC hybrid system coupled with thermal swing adsorption for H_2 purification: Parametric and exergy analyses. Energy Convers Manage 2018;174:802–813.